REPORT DOCUMENTATION PAGE

AFRL-SR-AR-TR-04-

0214

1. AGENCY USE ONLY (*Leave Blank*)	2. REPORT DATE	3. REPORT TYPE AND DATES COVERED
	2 April 2004	1 December 2001- 31 December 2003

4. TITLE AND SUBTITLE
Optical Supramolecules for Chemical & Physical Sensing

5. FUNDING NUMBERS
F49620-01-1-0118

6. AUTHORS
Daniel G. Nocera

7. PERFORMING ORGANIZATION NAME(S) AND ADDRESS(ES)
Massachusetts Institute of Technology
Department of Chemistry
77 Massachusetts Avenue
Cambridge MA 02139

8. PERFORMING ORGANIZATION REPORT NUMBER

9. SPONSORING / MONITORING AGENCY NAME(S) AND ADDRESS(ES)
Lt. Col. Paul C. Trulove, Ph.D.
AFOSR/NL
801 North Randolph Street, Room 732
Arlington VA 22203-1977

10. SPONSORING / MONITORING AGENCY REPORT NUMBER

11. SUPPLEMENTARY NOTES

12a. DISTRIBUTION / AVAILABILITY STATEMENT

Approve for Public Release: Distribution Unlimited.

12b. DISTRIBUTION CODE

13. ABSTRACT (*Maximum 200 words*)

This proposal seeks to bring to the AFOSR a strategy to use bio-inspired concepts of recognition and signal transduction to unite the areas of optical chemosensing and nanoscience to address diverse chemical and physical sensing needs of the United States Air Force. Luminescent molecule, supramolecule or materials have been synthesized for targeted sensing application. An intrinsic component of the program has been to define fundamental parameters that control the nonradiative and radiative energy flows so that the luminescence intensity and lifetime of the optical probe may be used for signal transduction. The following major achievements have been made by the research program (1) the development of the first microfluidic chemosensor for the detection and monitoring of chemical species of relevance to the Air Force on especially small length scales; (2) the development of new optical probes for accurate temperature and pressure measurements at aerodynamic surfaces; and (3)the development of new materials for an optical diagnostic technique that we invented to detect and measure turbulence. Achievements (1)-(3) have been transitioned to several research efforts in Air Force laboratories.

14. SUBJECT TERMS
Chemosensors, luminescence, supramolecule, nanoscopic, microfluidic
Optical diagnostics, molecular tagging velocimetry (MTV)
Pressure sensitive paints (PSPs), temperature sensitive probes (TSPs)

15. NUMBER OF PAGES
11

16. PRICE CODE

17. SECURITY CLASSIFICATION OF REPORT	18. SECURITY CLASSIFICATION OF THIS PAGE	19. SECURITY CLASSIFICATION OF ABSTRACT	20. LIMITATION OF ABSTRACT
UNCLASSIFIED	UNCLASSIFIED	UNCLASSIFIED	SAR

NSN 7540-01-280-5500

Standard Form 298 (Rev. 2-89)
Prescribed by ANSI Std. Z39-1
298-102

Table of Contents

1. Executive Summary

Proposal F49620-01-1-0118 seeks to bring to the AFOSR a strategy to use bio-inspired concepts of recognition and signal transduction to unite the areas of optical chemosensing and nanoscience to address diverse chemical and physical sensing needs of the United States Air Force. Luminescent molecule, supramolecule or materials have been synthesized for targeted sensing application. An intrinsic component of the program has been to define fundamental parameters that control the nonradiative and radiative energy flows so that the luminescence intensity and lifetime of the optical probe may be used for signal transduction. The following major achievements have been made by research program F49620-01-1-0118: (1) the development of the first microfluidic chemosensor for the detection and monitoring of chemical species of relevance to the Air Force on especially small length scales; (2) the development of new optical probes for accurate temperature and pressure measurements at aerodynamic surfaces; and (3) the development of new materials for an optical diagnostics technique that we invented to detect and measure turbulence. Achievements (1) - (3) have been transitioned to several research efforts in Air Force laboratories. Below is a description of our progress in each of these areas. Each section concludes with a description of transition to the DoD laboratory or related program that was impacted by the results emanating from F49620-01-1-0118.

Two graduate students and a two postdoctoral associates have performed the chemistry, materials science, bio-conjugate chemistry and optical and laser spectroscopy that is at the core of this research program. Dr. *Christina Rudzinski* graduated with her Ph.D. in July 2001 [*2.4.1*]. She was responsible for much of the work reported in Sections 2.1 (3R chemosensing, $[Re_6Q_8]^{2+}$ photophysics and μFOC). She is the project leader for the DoD project team on chem- and biowarfare sensing projects at Lincoln Labs; the work is supported by the US Army, DARPA, Joint Program Office for Biological Defense and the Office of the Secretary of Defense.

Ms. *Aetna W. Wun*, who hails from the University of California at San Diego, stepped into the position vacated by Dr. Rudzinski. Ms. Wun is well versed in chemical and materials synthesis, she complements this expertise with a sound knowledge of optics and laser spectroscopy. She has been responsible for advancing the work of Dr. Rudzinski by using bio-inspired concepts of molecular recognition on nano- length scales. She also performed the work described in Section 2.3.

Dr. *Glen Walker* entered this AFOSR program from Nathan Lewis' labs at Caltech where he worked on the electronic nose sensing project. Glen was primarily responsible for the synthesis and photophysical characterization of tracers in the PSP and MTV projects described in Section 2.2.

Upon his departure from MIT, his position was filled by Dr. *Thomas Gray*. Preston graduated from Harvard (Ph.D., Chemistry, 2001). He is an expert in the design of all inorganic excited states. He prformed the work described in Section 2.1.2.

Ms. Emily Meyer was an undergraduate majoring in Physics. She graduated from MIT in 2000 (S.B.) [*2.4.2*]. Her undergraduate thesis focused on defining the photophysics mechanisms of excited states.

2. Technical Summary of Work Accomplished

A benchmark of this program is the development of "3R" – recognize, relay, report – chemosensing. A major goal of the previous funding cycle was to implement 3R chemosensing on microfluidic length scales. In this section, new advances in the fundamental science and application of 3R chemosensing will be described. The section concludes with a summary of our design of the first microfluidic optical chemosensor.

2.1. 3R Chemosensing

2.1.1. Mechanistic Studies

The basic 3R approach is schematically outlined in Figure 1 [*2.4.3*]. A non-covalent molecular recognition event at the receptor site is communicated, by physical or chemical means, to a reporter site, which produces a measurable signal. A rapid equilibrium between the analyte and the receptor site affords the chemosensor a real-time response that varies with analyte concentration. We have applied the 3R approach to detect chemical signatures of jet fuels for field monitoring and environmental remediation at United States Air Force bases and storage facilities. The evolutionary members of the chemosensors designed for this application are shown in Figure 2. In our design, a cyclodextrin (CD) was used as the recognition site, a terbium ion (Tb^{3+}) was the reporting site, which was excited by an energy transfer relay from the mono- or bicyclic polyaromatic hydrocarbon (PAH). β-CD (7 D-glucose rings composing the bucket) binds BTEXs (benzene, toluene, ethylbenzene, xylene) and bicyclic aromatics (e.g., naphthalene, biphenyl) but not larger polyaromatics. Because we were interested in total aromatic content for the Air Force, β-CD proved to be the ideal receptor site for our targeted chemosensing application.

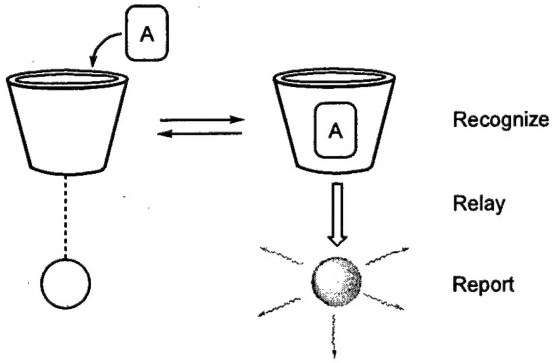

Figure 1. *The 3R scheme used for chemosensor development. A = analyte.*

An important design element of the chemosensors in Figure 2 is that the luminescent signal is triggered upon recognition of analyte by the CD. Thus the presence of PAH is detected by a visible signal against a dark background. Of the chemosensors shown in Figure 2, **3** possesses the most ideal properties for eliciting a triggered signal upon PAH recognition for the reasons presented in our recent review of the subject [*2.4.3*]. Because **1-3** pre-date the previous funding period, these molecules will not be discussed further. However **4** represents a new chemosensor from the previous funding cycle that was developed to contribute critically to our understanding of the relay mechanism [*2.4.4*].

Chemosensor **4** was prepared by the method outlined in Scheme 1. The methodology permits the distance between the Tb^{3+} reporter site and CD binding site to be increased with respect to **3** while maintaining the same regiochemistry. Despite comparable binding of PAHs to **3** and **4** and identical coordination spheres (neither has water coordinated to the Tb^{3+} ion as established by Horrock's photophysical method), the latter produces a triggered signal with a dramatically reduced intensity (by a factor of 16) for model PAHs such as biphenyl. Moreover, time-resolved measurements (Figure 3) show that the appearance of Tb^{3+}

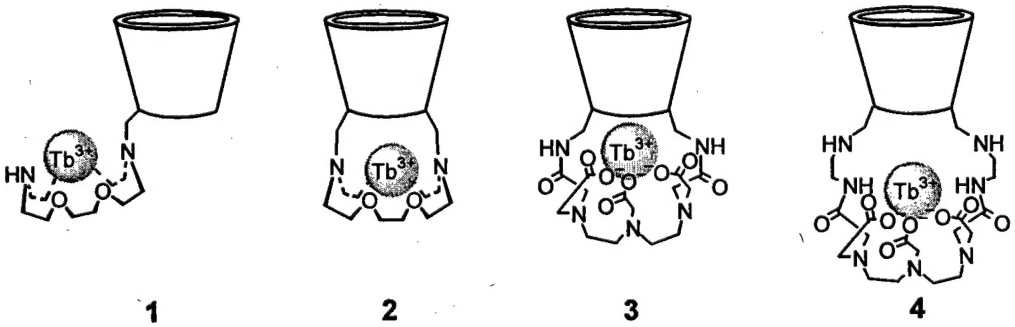

Figure 2. *Different chemosensors designed for the detection of PAHs by the 3R approach.*

Scheme 1

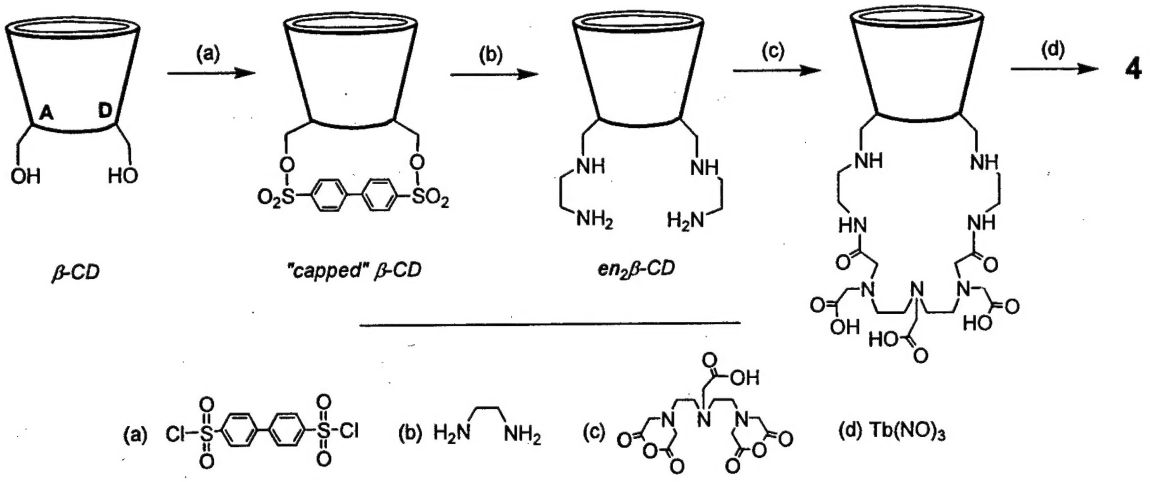

emission from **4** appears on a timescale that is twice as slow as that observed from **3**; both exhibit the natural decay lifetime of 1.6 ms for the Tb^{3+} ion. A thorough analysis of these data establishes that the energy transfer mechanism is Dexter and not Förster (due to the low absorption cross-section of the $^7F_J \rightarrow {}^5D_4$ transition of the Tb^{3+} ion). A Dexter treatment of these time-resolved energy transfer kinetics predicts the donor-acceptor distance in **4** to increase by 1.8 Å, a distance that is concordant with the distance measurements from energy minimized molecular modeling calculations. Moreover, simple bond length calculations for the added ethylenediamine (en) spacer place the binding site for **4** 1.95 Å further away than that for **3**. The differences in the energy transfer rate constant, k_{en}, between **3** and **4** are thus accounted for by the change in donor-acceptor separation, ΔR_{DA}. However, the energy transfer rates does not solely account for the ×16 difference in luminescence intensity of the two chemosensors. Increasing distance also causes a decrease in spin-orbit coupling interaction,

$$H_{SO} = \sum \frac{Ze^2}{4m^2c^2}\left(\frac{1}{R^3}\right)\ell \cdot s \qquad (1)$$

where Z is the atomic number, m is the mass, ℓ and s are the orbital and spin angular momentum

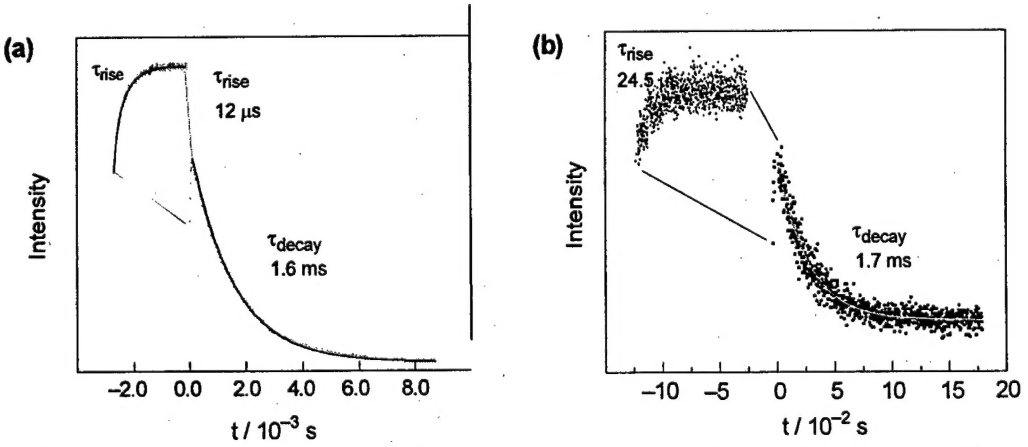

Figure 3. *The growth and subsequent decay of Tb^{3+} luminescence (λ_{em} = 546 nm) from (a) **3** and (b) **4** upon the excitation of biphenyl with the fourth harmonic of a Nd:YAG nanosecond laser (λ_{exc} = 273 nm). The exponential fits of the data, from which the risetime and decay rate constants were derived, are displayed by the solid lines.*

operators, respectively. This is an important contributing factor to chemosensor function because the initially prepared $^1\pi\pi^*$ excited state of the PAH is too short-lived to participate in energy transfer. The Tb^{3+} ion facilitates intersystem crossing to the $^3\pi\pi^*$ whereupon energy transfer occurs to produce the $^5D_4$ emissive excited state of the Tb^{3+} ion. The increase in R_{DA} for **4** is manifested in a smaller yield of $^3\pi\pi^*$ and thus less intense emission upon PAH recognition. This result serves to highlight a little recognized feature in the signal transduction pathways of optical chemosensors, especially those involving Tb^{3+} ions as the light-emitting center. In addition to the obvious importance of the Tb^{3+} ion as the emitting center in the energy transfer process, the Tb^{3+} ion also provides a mechanism to produce a long-lived donor excited state from which energy transfer may occur. In the absence of this heavy atom effect, the singlet-excited state of the aromatic would return to its ground state before energy transfer could occur. By channeling the singlet to a long-lived triplet, ample time is provided for the slower energy transfer process to effectively compete with the fast natural radiative and nonradiative processes of the analyte.

2.1.2. New Excited States

A fundamental activity of this program is the discovery and elucidation of new excited states. For the purposes of the proposed research effort, we became interested in the developing intense luminescent dyes of exceptional chemical and optical stability. Our attention turned to all inorganic clusters $[Re_6Q_8L_6]^z$ (Q = S, Se; L = σ-donor ligand), which are solely composed of stable metal-metal and metal-chalcogenide bonds. The structures of these clusters, shown in Figure 4, consist of an octahedral metal core coordinated by eight-face bridging X or Q ligands and six axial L donor ligands. They exhibit exceptional thermal stabilities, as they are prepared from high temperature liquid melts (600-800 °C). Upon UV-visible excitation, they emit brilliant red phosphorescence with microsecond length lifetimes. The promise of these clusters as dyes for sensor constructs provided an impetus for understanding the fundamental factors controlling their excited state properties. We undertook a detailed study of the electronic structure, photophysics and vibrational spectroscopy of 24 $[Re_6S_8]^{2+}$ and $[Re_6Se_8]^{2+}$ with the goal of precisely defining the nonradiative decay mechanism in these clusters [*2.4.5*, *2.4.6*]. The principle findings from this work are as follows.

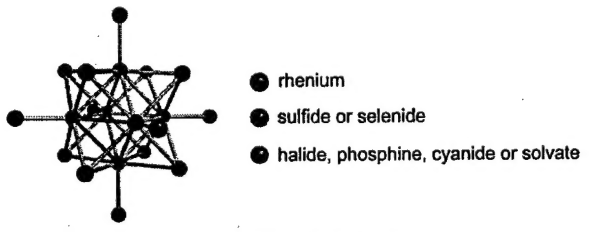

Figure 4. *Structure of $[Re_6Q_8L_6]^z$ (Q = S, Se; L = σ-donor ligand) clusters.*

(a) Room-temperature luminescence lifetimes of the clusters in fluid solution range from 2-22 μs, and quantum yields, from *ca.* 1-22%. Solid-state emission lifetimes and quantum yields occupy a similar range at room temperature.

(b) The long lifetimes, large Stokes shifts and excited-state quenching by O_2 indicate an emitting excited state with considerable spin-triplet character. This was confirmed by electronic structure calculations of the lowest energy excited state.

(c) Those species with oxygen donor ligands deliver maximal quantum yields, the longest lifetimes, and the highest energy emission. Conversely, clusters having six soft, polarizable ligands, such as iodide, emit with less intensity, shorter life spans, and redder luminescence.

(d) $[Re_6S_8]^{2+}$ and $[Re_6Se_8]^{2+}$ emission obeys the approximate energy gap law. This observation implies a common lumophoric kernel in $[Re_6Q_8]^{2+}$ (Q = S, Se) species. It also suggests that these clusters, once excited, share a common deactivation mechanism.

(e) Electronic structure calculations are consistent with energy gap law predictions. Quasi-relativistic electronic structure calculations indicate a lowest energy excited state parentage that is largely localized on the cluster core. These parentages are shown in Figure 5.

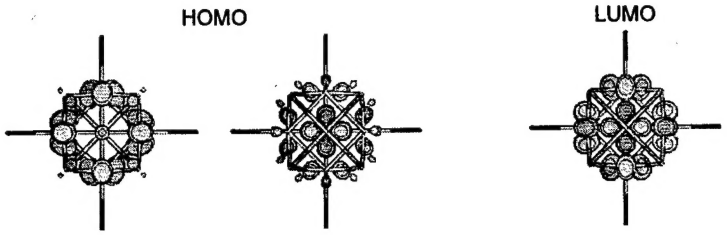

Figure 5. *Degenerate e_g HOMOs and a_{2g} LUMO calculated at the B3LYP/LANL2DZ level of theory.*

(f) Group theory predicts that, for a cluster of ^3E_g excited state parentage in O_h symmetry, deactivating vibrations span the A_{1g} and E_g irreducible representations. A normal mode analysis indicates three A_{1g} and six E_g modes that collectively involve the three shells of the cluster structure: the Re_6 octahedron, the S_8 cube of face-bridging chalcogenides, and the six axial ligands. The modes are shown in Figure 6.

(g) The calculated modes of (f) are all observed in single crystal Raman spectra in the low-frequency ($\leq$ 100 - 450 cm^{-1}) range. Polarization measurements identify the A_{1g}-symmetric breathing modes; the E_g vibrations were assigned by comparison with quantum chemical/normal coordinate calculations.

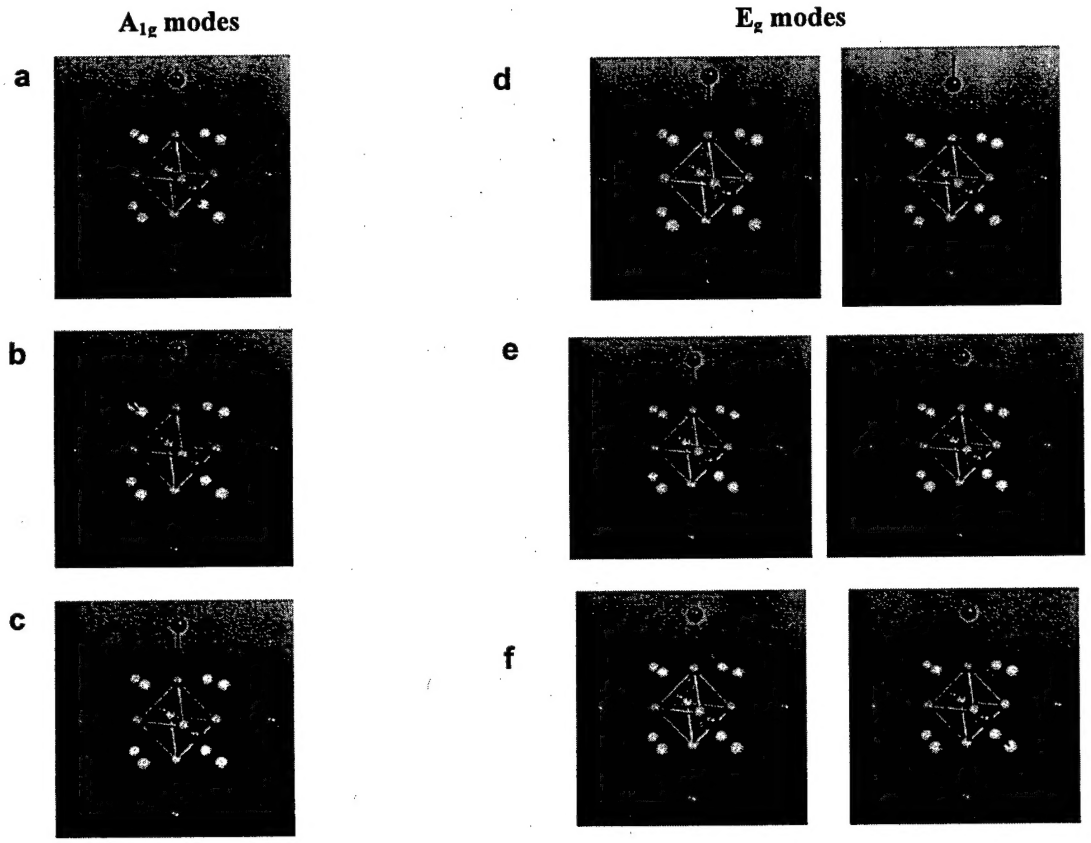

Figure 6. *The (a) $\nu_{a1g}(Re_6)$, (b) $\nu_{a1g}(S_8)$ and (c) $\nu_{a1g}(Cl_6)$ totally symmetric vibrational modes of $[Re_6S_8Cl_6]^{4-}$ and the E_g vibrations of $[Re_6S_8Cl_6]^{4-}$ at (d) 172 cm^{-1} ($\nu_{eg}(obsd)$ = 162 cm^{-1}), (e) 244 cm^{-1}, (calculated intensity is small, bands not observed) and (f) 302 cm^{-1} ($\nu_{eg}(obsd)$ = 277 cm^{-1}). Calculated frequencies were obtained from the HF/enhanced basis level of theory.*

(h) Analysis of the emission second central moment provides an effective deactivating vibrational frequency, $\hbar\omega_{eff}$, for individual clusters. The experimental range is ~150 - 350 cm^{-1}. This frequency span coincides with the vibrational energies of the $[Re_6Q_8]^{2+}$ kernel presented in (f), supporting the notion of a core-centered excited state. Substitution of the second-moment derived $\hbar\omega_{eff}$ into the approximate energy gap law reproduces the observed photophysical parameters. This observation affirms the validity of the second moment analysis.

(i) Clusters possessing axial phosphine, cyanide and solvate ligands possess modes of sufficient energy, for energy gap law purposes, to be discernible from other intracluster vibrations. Notwithstanding, these clusters obey the energy gap law correlation, indicating that the emitting excited state is insulated from vibrations of ligands attached to the emitting core at the axial coordination site.

(j) The structural transformation accompanying nonradiative decay of $[Re_6Q_8]^{2+}$ clusters was identified from temperature-dependent photophysical measurements and hybrid density-functional calculations to be tetragonally flattened ($D_{4h}(^3B_{1g})$) → octahedral ($O_h(^1A_{1g})$) singlet ground state. The activation energy for this transformation was experimentally determined to be ~1500-2000 cm^{-1}, which was reproduced from time-dependent DFT calculations. These findings concur with (e) - (i) since it is logical that core localized vibrations will be excited as the $[Re_6Q_8]^{2+}$ clusters dismount from the long-lived excited state to the ground state.

Our work constitutes the most comprehensive single study of metallocluster-based luminescence to date. The combined spectroscopic, computational and photophysical results show that long-lived and bright luminescence may be obtained as long as the $[Re_6Q_8]^{2+}$ core is unperturbed, regardless of the nature of the axial ligand. Thus the axial ligands provide handles for chemical modification of a cluster core that effectively constitutes a molecular light bulb. This result might be exploited in the use of these stable metal-metal bonded species as dyes for the amplification medium of lasing architectures needed for the constructin of nanosensors.

2.1.3. Micro-Fluidic Optical Chemosensor

MicroFluidic (μF) platforms have emerged as an important technology for chemo- and bioanalytical applications. The miniaturization offered by μF devices allows for the analysis of fluid samples to be performed on a chip, leading to advantages such as reduced sample volume, increased reaction speed and the possibility of massive parallelism. To date, optical analysis on μF platforms has been performed by direct spectroscopic detection methods. The advantages that 3R sensing offers over direct detection methods motivated us to investigate whether 3R function could be transferred to μF platforms. By combining organic and materials synthesis with lithographic patterning methods and undertaking both steady-state and time-resolved spectroscopy on patterned devices, we have shown during the past funding cycle that the complicated signal transduction mechanisms of the supramolecular optical chemosensors may be established in the microdomain. From the knowledge garnered from this effort, we have fabricated the first microFluidic Optical Chemosensor (μFOC) [*2.4.7*].

The realization of μFOCs demanded that a supramolecule architecture be incorporated into a matrix that is compatible with lithographic patterning protocols. Accordingly, a major thrust of our work was to develop methods to permit the attachment of the CD chemosensor onto a substrate. Many syntheses were explored and we were successful in incorporating **3** into organic and inorganic polymer matrices. The most successful films for μFOC detection were prepared according to the method shown in Scheme 2. The CD was condensed into a partially hydrolyzed tetraethylorthosilicate solution in ethanol (acid catalyzed conditions). This solution was spin-cast onto clean, dry, quartz substrate to give gel films of thicknesses ranging from 0.2 - 0.6 μm, as determined by profilometry measurements. Squares of these sol-gel films were photo-lithographically patterned within the serpentine channel of the device shown in Scheme 2. The device exhibits excellent optical response to polyaromatics; importantly, time-resolved

Scheme 2

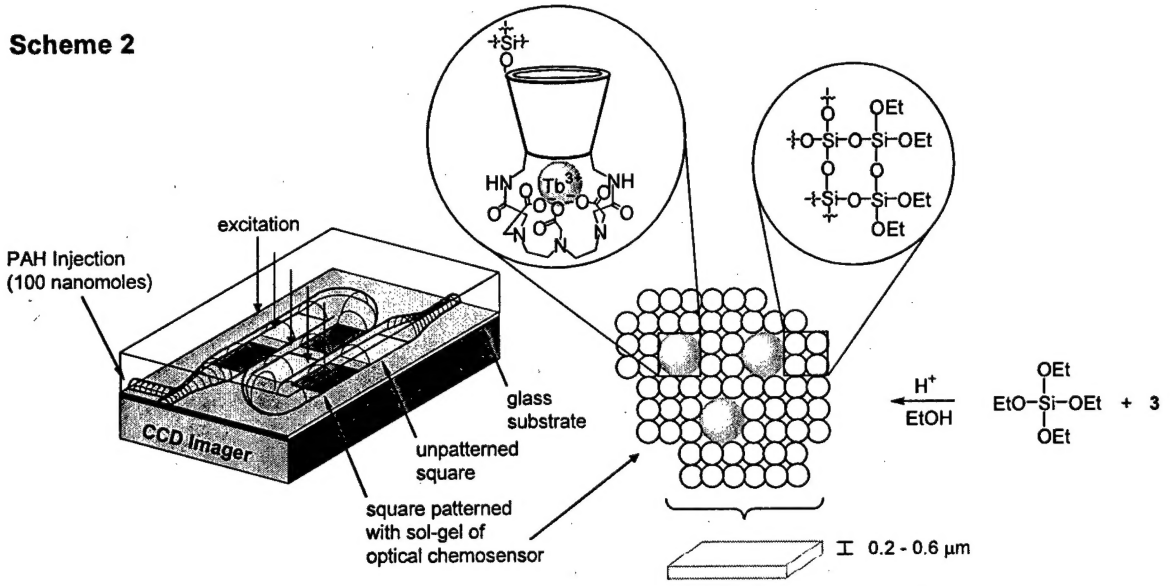

kinetics measurements on the sol-gel thin films established that the same 3R mechanism observed in solution prevails in the film. A 45-fold enhancement of the Tb^{3+} luminescence intensity is triggered when a 50 μM solution of biphenyl contacts the patterned microstructure. Equivalent concentrations of analyte added to aqueous solutions of **3** generate significantly smaller enhancements (e.g., 8-fold enhancement for [biphenyl] = 50 μM), suggesting that analyte associates more strongly to the CD bucket of **3** when immobilized in sol-gel films. The Tb^{3+}-luminescence enhancement proves to be concentration-dependent, increasing monotonically with the concentration of biphenyl; detection of biphenyl at 5 μM is easily achieved. We estimate from the extrapolation of these data to the limits of our detector response that analyte can be detected reliably to 100 nM. The μFOC platform exhibits considerable structural and optical integrity; the signal response of **3** is maintained over a period of greater than three months with little degradation of the signal response (<10% change in signal intensity).

2.1.4. A 3R Chemosensor Transition: An Anthrax Smoke Detector Operating on the Basic Principles of a 3R Detection Scheme

The anthrax attacks of 2001 have highlighted the need for new methods of detecting bioaerosols, especially airborne spores that carry anthrax (*Bacillus anthracis*). Current methods of bacterial spore (endospore) detection, such as colony counting and PCR, require trained personnel for sampling and analysis. Early warning detection systems are needed that are cheap, low maintenance and able to continually monitor while unattended. In response to this need, the 3R sensing strategy based on the Tb^{3+} luminescence of Section 3.1.1.1 has been transitioned to JPL for the development of an anthrax "smoke detector" (ASD). A former student from this AFOSR-sponsored research program and now a staff scientist at JPL, Dr. Adrian Ponce, has implemented the 3R Tb^{3+}-based sensing scheme to design, develop and test an ASD instrument capable of automated monitoring for airborne bacterial spores containing the anthrax bacteria.

The principle of operation of the ASD targets a unique chemical marker, DPA (2,6-pyridine dicarboxylic acid), contained within bacterial spores at high concentrations. When DPA is released into bulk solution by physical (microwave) lysing, it binds terbium ions with high affinity to set up the 3R energy cascade. An intense green luminescence is triggered under UV excitation, thus signaling the presence of bacterial spores. The intensity of the luminescence can be correlated to the number of

endospores per milliliter. Concentrations below 100 spores/liter of air trigger a response from the smoke detector in half the time it takes for a person to breathe in a lethal dose of anthrax spores. The ASD thus provides a simple and robust early warning system for the automated, continuous, long-term monitoring instrument of airborne anthrax spores.

The sensitivity of the ASD is primarily governed by the Tb^{3+}-DPA binding constant, which can be increased by the design and implementation of new Tb^{3+}-based receptor sites that exhibit cooperative binding towards DPA. This work will continue to be performed as a natural outgrowth of this AFOSR program. These new constructs will be transitioned from the laboratory bench of the PI's program to Ponce at JPL, who will incorporate them in next generation ASD prototypes.

2.2. Pressure and Temperature Sensing at Aerodynamic Surfaces

2.2.1. Quantum Dots as Temperature Probes for Pressure Sensitive Paints

Beyond the chemical environment, the Air Force faces challenges in sensing many different types of physical phenomena. The measurement of surface pressures in aerodynamics testing is especially prominent in Air Force efforts to design high performance aircraft and engines. Surface pressure measurements relying on the longstanding and conventional single-point "macroscopic" methods based on taps and transducers are being replaced with multi-point "molecular" methods based on the luminescence from pressure sensitive paints (PSPs). PSPs contain a luminescent probe that is sensitive to the concentration of oxygen in the coating; the luminescence variance arising from oxygen quenching within the paint allows for the creation of real-time optical maps of surface pressure variations on aerodynamic surfaces. A significant challenge to this technique is that the luminescence of the pressure probe is also invariably sensitive to temperature fluctuations. The temperature and pressure dependencies must be disentangled for the accurate measurement of pressure. The Air Force has initially addressed this problem by performing a separate temperature calibration run. However, owing to the significant expense of running wind tunnel facilities, the Experimental Operations and Diagnostics Branch of the Aeromechanics Division of the Flight Dynamics Directorate at Wright Patterson AFB, was interested in eliminating the temperature calibration run in its subsonic wind tunnel facility. We addressed this Air Force need by setting out to develop a luminescence "thermometer" that could be incorporated into PSPs currently used by the Air Force.

Our initial studies focused on using the metal-to-ligand charge transfer excited state of metal polypyridyls [*2.4.8*, *2.4.9*]. But our attention soon turned to nanocrystalline CdSe particles encapsulated by a passivating layer of ZnS. This line of work was greatly facilitated by the informal collaboration between the PI and his colleague, Professor Moungi Bawendi, who leads a preeminent program in nanocrystal research. We have shown that (CdSe)ZnS quantum dots (QDs) possess extremely attractive properties for application as temperature sensitive probes (TSPs) [*2.4.10*, *2.4.11*]. The emission mechanism of the QDs involves electron-hole recombination within the inorganic core of the particle, which is insensitive to collisional quenching by oxygen. Hence the temperature profile of bilumophoric coatings containing (CdSe)ZnS QDs and a pressure sensitive probe is provided directly from monitoring the luminescence of the dots. Figure 7 shows the temperature dependence of the emission band for (CdSe)ZnS QDs. Spectra were recorded at intervals throughout the temperature range of 5-40 °C. The linear change in emission intensity of 1.5% per °C throughout the entire 35 °C range far exceeded Air Force design specifications by 0.5% per °C. The exceptional photostability of the QDs and the reversibility of the luminescence change with temperature are in evidence from the almost perfect superposition of the 25 °C-emission bands of Figure 7 recorded at the beginning, middle, and end of the experiment. As expected, the QD luminescence showed absolutely no dependence on oxygen concentration.

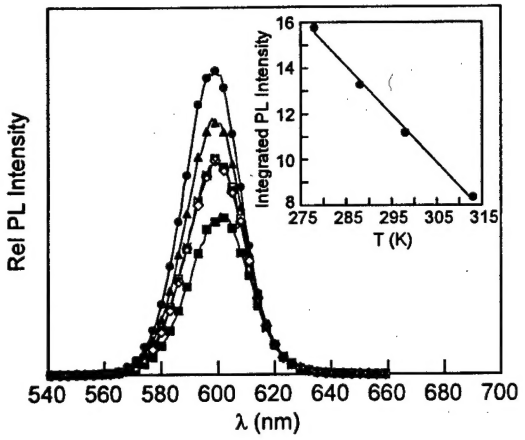

Figure 7. The photoluminescence emission spectra for polymer supported (CdSe)ZnS QDs excited at 480 nm at near ambient temperatures in the following order: 298 (×), 313 (■), 298 (Δ), 288 (▲), 278 (●), 298 K (◊). Inset: variation in integrated photoluminescence emission intensity with temperature and a least-squares linear regression analysis of the data.

The QDs provide additional conveniences for the design of pressure- and temperature-sensitive bilumophoric coatings. The near-Gaussian emission band of narrow widths (fwhm = 30 nm) may be produced across the full range of the visible spectrum (400 nm (15 Å nanocrystals) - 700 (100 Å nanocrystals)); accordingly the position of the emission band for luminescence thermometry can be easily tuned away from the emission band used for pressure measurements. At the same time, the QDs possess a very broad and featureless absorption profile with an extinction coefficient that is essentially invariant from 300 to 480 nm. Thus the QD emission needed for thermometry measurements may be achieved with excitation wavelengths that are coincident with excitation of the pressure-sensitive lumophore. Finally, the (CdSe)ZnS QDs were incorporated into PSP binders with the same preparative conditions used to formulate PSPs under study and use at Wright Patterson Labs.

2.2.2. Quantum Dot TSP Transition to Wright Patterson Labs

The significant temperature dependence of the luminescence combined with its insensitivity to quenching by oxygen establishes these (CdSe)ZnS-based materials as an attractive new class of optical indicators for luminescence thermometry applications. The QD-based technology was directly passed from this AFOSR program to the Aerodynamics Configuration Branch (AFRL/VAAA) of the Air Vehicles Directorate at Wright Patterson Air Force Base for testing and evaluation. This transition was made possible by an STTR involving Innovative Scientific Solutions, Inc. (ISSI), a sub-contractor to the Air Force. All expectations of the QDs as temperature probes were confirmed at Air Force facilities in 6.2 tests. The results of this work have been described in a recent joint publication from the PI labs, AFOSR and ISSI [*2.4.11*]. We hope that QD paints containing (CdSe)ZnS QDs as TSPs will be commercialized in 6.3 ventures at Arnold and Wright Patterson AFB over the next two years.

2.3. Development of the MTV Technique for the Micro-/Nanodomain

The quantitative measure of turbulent flows at aerodynamic boundaries is another physical sensing problem that has occupied this research program. We have invented an optical technique called Molecular Tagging Velocimetry (or MTV) [*2.4.12* and *2.4.13*], which allows us to physically sense flow by precisely describing the velocity profile of a fluid. In the MTV experiment, luminescent supramolecular tracers are dissolved in a fluid gas or liquid and a grid of laser lines is imposed upon the flow by shining a laser beam off of a grating to produce a glowing grid, defined by the luminescence from the optical supramolecule tracer. The tracer must exhibit a bright, non-quenchable luminescence, which is sufficiently long-lived to convect with the flow (μs to ms depending on the fluids problem). The deformation of the grid as it moves with the flow is recorded with a CCD camera. By measuring the distance and direction each grid intersection travels and knowing the time delay between each image, the two velocity components in the grid plane may be determined (the out-of-plane velocity can be determined with a second CCD camera). Parameters important to the fluid physicist, such as turbulence intensities, the Reynolds stress and vorticity may be calculated.

Prior to the previous funding period, supramolecular tracers developed in our labs enabled us to image flows to 50 ms. However, many interesting flow structures, including those on micro- and nano-dimensions, move at much slower speeds (especially near boundary walls). To advance the MTV technique to the micro-/nano-dimension, we became interested in using photoactivated dye tracers that could be *reversibly* caged and decaged.

We sought to develop dyes based on principles previously established by Mann and co-workers in their studies of $CpRu^{II}$ arene and aromatic dye complexes in nonaqueous solutions. In this design, a dye complexed to the metal head-group does not luminesce since the excited state will decay nonradiatively via the low-lying ligand field states of the metal head group. If the ligand field state is dissociative with respect to ligand, then laser excitation of the complex frees the laser dye from the metal complex. As applied to the MTV technique, once liberated from the deactivating head group, the laser dye is free to emit upon delivery of a second excitation pulse to image the dye. The luminescent dye can be tracked indefinitely by simple fluorescence imaging approaches with a second interrogating laser pulse (or other source to illuminate the flow field). The image is produced by the exciting laser pattern; a fluorescent dye is spatially produced only in regions where the laser has excited the fluid.

In our studies, we found that the Mann chemistry does not translate to aqueous solution because the $18e^-$ aquo complex, $[CpRu^{II}(H_2O)_3]^+$, produced upon dye liberation was too stable. We thus sought to labilize the coordinated waters so that the freed dye could re-attach to the metal head group, thus making the system reversible. Use of $Cp^*Ru^{II}(MeCN)_3^+$ as a starting material has proved to be convenient in the synthesis of the two caged dye complexes shown in Figure 8. Both compounds have been isolated and characterized by x-ray crystallography. Interestingly, the acridone (PSA) complex is a dimer formed from the attachment of the Cp^*Ru^{II} head group to opposite faces of the acridone dye. This result is obtained owing to the presence of two phenyl groups in the acridone ring system. The dimer problem is eliminated when only one phenyl group is present in the dye ring system as exemplified by the caged coumarin (C460) complex. Both complexes are stable in air and water.

The dyes, shown in Figure 8, function as reversible photocaged tracers for the MTV technique. Photolysis of both complexes, which are initially non-emissive, with 305 nm light frees the dye. This process has been confirmed by UV-vis absorption and emission spectroscopy. The luminescence of the freed dye is intense and easily imaged by the MTV technique [*manuscript in preparation*]. We are currently implementing the tracers for the measurement of flows in small channels. As a technique/instrument development activity, the research has deviated far from the thematic "sensing" focus of this AFOSR program. Consequently, MTV work on small length scales will not be continued as part of this research program, though the instruments and techniques developed may be applied to the study of the any new devices developed on nano- length scales.

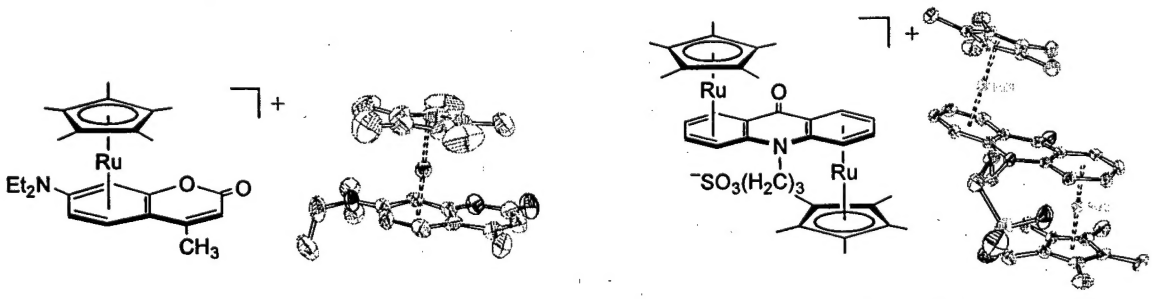

$Cp^*Ru(C460)^+$ **$(Cp^*Ru)_2(PSA)^+$**

Figure 8. *Isolation and structural characterization of new, reversible, caged dye tracers for application of the MTV technique to measure slow flows in microfluidic devices.*

2.4. List of Publications from Previous Grant Cycle

1. "Rational Design of Optical Sensors Through Control of Molecular Excited State Dynamics"; Christina M. Rudzinski, Ph.D. Thesis, Massachusetts Institute of Technology, **2001**.

2. "Photophysics of $[Re_6S_8]^{2+}$ Cluster Compounds" Christina M. Rudzinski, S.B. Thesis, Massachusetts Institute of Technology, **2000**.

3. "Buckets of Light"; Christina M. Rudzinski and Daniel G. Nocera, in *Optical Sensors and Switches*; V. Ramamurthy and K. S. Schanze, K. S. (Eds.); Molecular and Supramolecular Photochemistry, vol. 7; Marcel Dekker: New York, **2001**, p. 1-91.

4. "Optimized Detection of Aromatic Hydrocarbons in Aqueous Solution by Lanthanide-Ion Modified Cyclodextrin Supramolecules"; Christina M. Rudzinski, Scott D. Carpenter and Daniel G. Nocera, submitted to *Chem. Eur. J.*

5. "Spectroscopic and Photophysical Properties of Hexanuclear Rhenium(III) Chalcogenide Clusters"; Thomas G. Gray, Christina M. Rudzinski, Emily E. Meyer, R. H. Holm and Daniel G. Nocera, *J. Am. Chem. Soc.* **2003**, *125*, 4755-70.

6. "Excited-State Distortion of Rhenium(III) Sulfide and Selenide Clusters"; Thomas G. Gray, Christina M. Rudzinski, Emily E. Meyer and Daniel G. Nocera, *J. Phys. Chem.* **2004**, ASAP, Web Release Date: 23 March

7. "A Supramolecular Microfluidic Optical Chemosensor"; Christina M. Rudzinski, Albert M. Young and Daniel G. Nocera, *J. Am. Chem. Soc.* **2002,** *124*, 1723-7.

8. "Compounds of general interest. A luminescent complex of Re(I): fac-$[Re(CO)_3(bpy)(py)](CF_3SO_3)$ (bpy = 2,2′-bipyridine; py = pyridine). Erick J. Schutte, B. Patrick Sullivan, Christopher J. Chang and Daniel G. Nocera, Inorg. Synth. **2002**, *33*, 227-30.

9. "$[Ru(4,7\text{-diphenyl-}1,10\text{-phenanthroline})_3]Cl_2$"; Glen W. Walker and Daniel G. Nocera, *Inorg. Synth.* **2004,** in press.

10. "Quantum dot optical temperature probes"; Glen W. Walker, Vikram C. Sundar, Christina M. Rudzinski, Moungi G. Bawendi and Daniel G. Nocera, *Appl. Phys. Lett.* **2003**, *83*, 3555-7.

11. "Temperature-Sensing Composition"; Alfred A. Barney, Moungi G. Bawendi, Vikram C. Sundar, Daniel G. Nocera, Christina M. Rudzinski and Glen W. Walker, Application filed by MIT on 9 February 2001 (serial number 09/779,437); MIT Internal Case #8800 (2001). U.S. Pat. Appl. Publ. 2002110180, **2002**.

12. "Investigation of Advanced Luminescent Probes and Paint Architectures"; Gary A. Dale, Larry P. Goss, Neal A. Watkins, Daniel G. Nocera, *Proc. Int. Instr. Symp.* **2001**, *47*, 10-25.

13. "Molecular Tagging Velocimetry Maps Fluid Flows"; Manooch M. Koochesfahani and Daniel G. Nocera, *Laser Focus* **2001**, *37(6)*, 103-8.

14. "Molecular Tagging Velocimetry: A Review of Techniques, Chemical Concepts, and Applications"; Manoochehr M. Koochesfahani and Daniel G. Nocera, *Exp. Fluids* **2004**, to be submitted.